INSTITUTO SUPERIOR TÉCNICO

PROJECTO MEFT

Control of a Robotic Leg for Walking, Running and Hopping in Irregular Surfaces

---

Author:
Nuno TEIXEIRA

Supervisor:
Dr. Rui DILÃO

Research work performed for the Master in Engineering Physics

at

NonLinear Dynamics Group
Physics Department

January 9, 2019

1 Introduction

One of the key factors that distinguish humans from other primates is that they are capable of having a bipedal walking/running gait. This aspect served as an evolutionary remark towards our movement because humans could have a much higher mobility aswell as having a bigger vision range than before against their preys and it's predators. This along with the development of technology allowed for humans to have a bigger advantage against natural conditions and therefore contributed for our survival as species. Since the way we walk is unique and very complex [10] regarding the rest the animal kingdom, a push has been made to reproduce the same type of walking and running in robots and other types of machines.

To accomplish the goal of imitating the same pattern of human walking and running, [8] describes that in the seventeenth century, Giovanni Afonso Borelli wrote "De motu Animalum", the first treatise on biomechanics, where he compared walking with vaulting over stiff legs although, while for running, he declared that the rebounding effect on compliant legs was important [4]. In an attempt to reproduce the same effects of human walking and running two models were created with entirely different dynamics. Walking was developed by [1, 10, 6] as a inverted pendulum model, while running was devolped by [3, 9], as a spring-mass model. With these models, several properties could be obtained such as the kinetic and potential energies, the speed and frequency as well as other aspects for the associated gait. The spring-mass model was able to explain the basics of running, although, regarding walking , it was verified this type of gaiting could not be imitated by using an inverted pendulum model [7]. One of the differences between the model and the experimental data points, for example, was the M shaped ground reaction force that is not present in the inverted pendulum model since delta functions appear at the beggining and ending of one step [11].

With this in account, [8] proposes a two compliant leg model consisting of two springs attached to a mass, being able to reproduce the same effects of walking with a relatively simple description despite the large complexity of the movement. In this paper, the stable parameter map is determined in relation with the variation of physical parameters such as the spring stiffness k. Also, it is shown that walking and running can be encapsulated into the same model with the energy associated to the system being the mediator between one type and the other type of gaiting. After the success, [12] uses the same model to determine 5 types of walking gaits, as well as to test the robustness of the model by determining the regions of attraction along with the saddle region associated to the parameter space.

2 State Of The Art

2.1 Running/hopping model

Starting with [3] a running/hopping model is analysed. In this model a spring-mass system is introduced by connecting the Center of Mass (CoM) of a robot to a massless spring. This system describes the dependency of the different physical variables that charecterize running/hopping. Hopping forward can be described by a non-linear system of equations described by an inverted pendulum spring propagating forward in which there are two phases, the ground phase,

$$\ddot{x} = x\omega^2 \left(\frac{l}{\sqrt{x^2 + y^2}} - 1 \right), \tag{1}$$

$$\ddot{y} = y\omega^2 \left(\frac{l}{\sqrt{x^2 + y^2}} - 1 \right) - g, \tag{2}$$

and the aerial phase, where,

$$\ddot{x} = 0, \tag{3}$$

$$\ddot{y} = -g. \tag{4}$$

In this system, m is the mass, $\omega^2 = \frac{k}{m}$ is the natural frequency of the spring, g is the gravitational acceleration, x is the horizontal displacement, y is the vertical displacement and $l = \sqrt{x_0^2 + y_0^2}$ is the rest length of the spring.
Fig. (1) helps to illustrate the model presented. In this figure, the spring touches the ground, starting the ground phase, with an angle of atack α, with an initial velocity $\vec{v}$ where β is the angle that the velocity makes with the ground. After the spring touches the ground, is compressed in the normal direction, and at the same time, mass propagates forward becouse the spring rotates around it's pivot point in the ground. After the spring reaches the same height as when it first touched the ground, it starts the aerial phase where the spring becomes disconnected from the ground until the mass reaches an height of $l \cos \alpha$ restarting the ground phase.

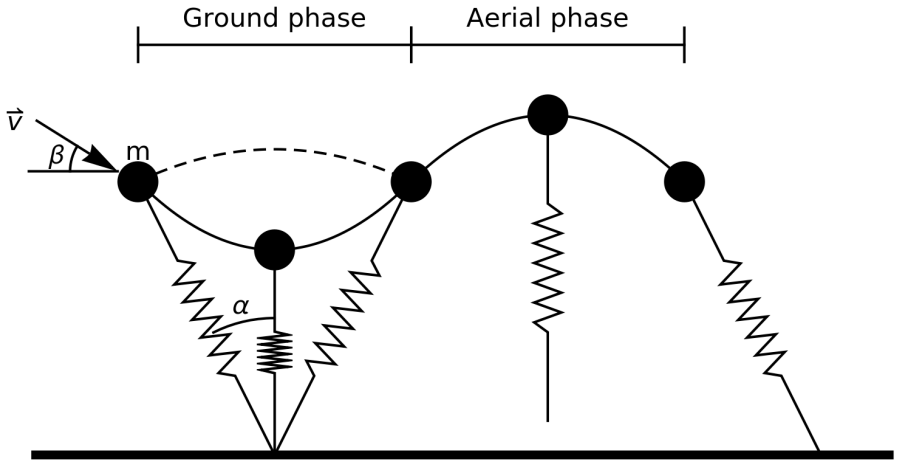

FIGURE 1: Running/hopping model described in [3]. This model displays the basic dynamics of running, it is charecterized by two phases, the ground phase and the aerial phase. The angle which the leg returns to the ground is the same as in the previous step. In this scheme, $\vec{v}$ is the velocity, m is the mass, α is the angle of attack.

The determination of the physical solutions are determined by narrowing the range of the parameters studied within the set of possible solutions. With this parameters, we need a small subset of them, the vector of landing velocity and leg length in this model to determine the state of the system and it's evolution. Since this is a physiological model, some of the parameters cannot be changed. Regarding running, an human subject maximizes the amount of energy that can be stored and delivered elastically [3]. This can be achieved by maximizing the contact length and this is why animals use flat angles on the landing velocities.

2.2 Walking model

Analysing [8], a model of two compliant legs is proposed. In this model, when one leg is on the ground, the system is equivalent to a inverted spring pendulum, this is called the single support phase. When the model is not in a single support phase, it is in a double support phase, where the two springs in this phase influence the movement of the CoM at the same time, reproducing a bipedal spring-mass walking. The springs accumulate and deliver energy so that the system remains convervative with no energy losses.
In single phase support, the dynamics of the center of mass (CoM) is as follows,

$$\ddot{x} = \frac{F_1}{m}\frac{x - x_{t1}}{l_1}, \tag{5}$$

$$\ddot{y} = \frac{F_1}{m}\frac{y - y_{t1}}{l_1} - g, \tag{6}$$

where (x, y) are the coordinates of the center of mass (CoM and (x_{ti}, y_{ti}) are the coordenates of the respective toes for the leg 1 and leg 2. With double support, the dynamics are similar to the previous case with the difference that we are in the presence of two springs, this is,

$$\ddot{x} = \frac{F_1}{m}\frac{x - x_{t1}}{l_1} + \frac{F_2}{m}\frac{x - x_{t2}}{l_2}, \tag{7}$$

$$\ddot{y} = \frac{F_1}{m}\frac{y - y_{t1}}{l_1} + \frac{F_2}{m}\frac{y - y_{t2}}{l_2} - g, \tag{8}$$

with F_i being the force applied on the mass by the respective leg,

$$F_i = k(l_0 - l_i) \geq 0 \quad i = 1, 2\,, \tag{9}$$

l_0 is the natural length of the spring, l_i is the respective length,

$$l_i = \sqrt{(x - x_{ti})^2 + (y - y_{ti})^2} \quad i = 1, 2\,. \tag{10}$$

Fig. (2) illustrates the model, single support to double support transitions occur when the center of mass drops to a height of $y \sin \alpha$ where α is the angle of attack and the vertical velocity is negative. Double support to single support transitions occur when the spring deflection $l_0 - l_i$ of one of the legs return to 0.

Let the Poincaré section be defined as the vector $\psi_n = (y_n, \beta_n)^T$ at the Vertical Leg Orientation (VLO). Everytime the system is in the single support phase and the leg is in it's vertical position we record the height of the CoM, y_n and the angle that the velocity makes with the ground, β_n. This state of the system defines the **stride** n of the simulation. Alternatively a **step** is defined when the system passes from single support to double support.

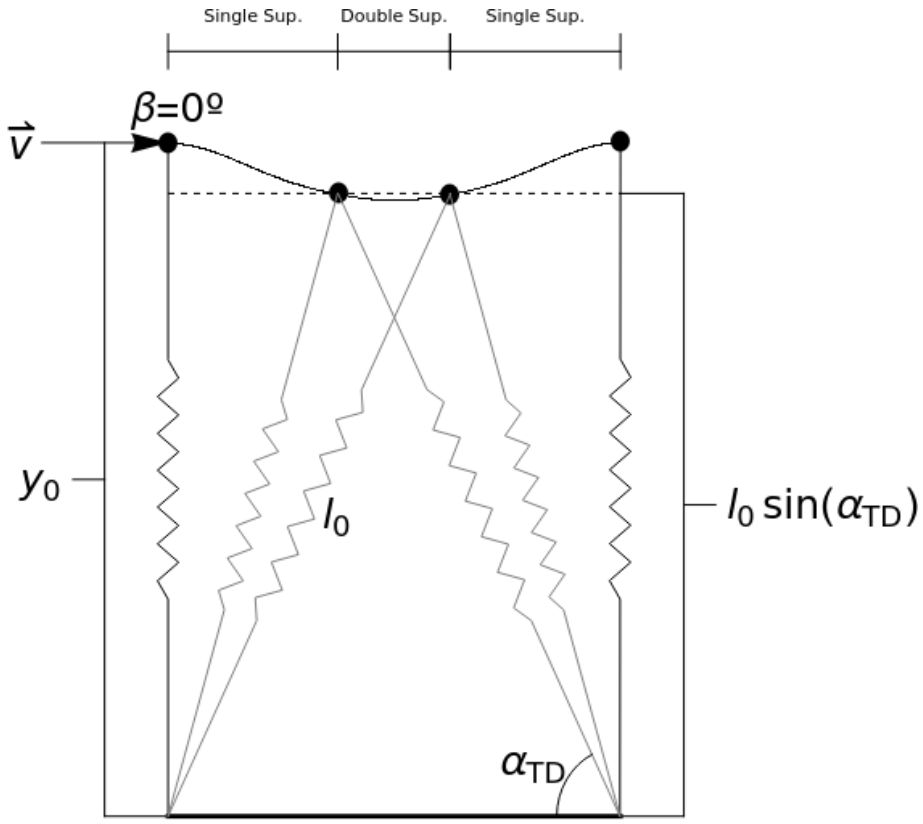

FIGURE 2: Bipedal spring-mass walking model described in [8]. The initial velocity is given by $\vec{v}$, in this case, $\beta = 0$, this is the velocity is initially parallel to the ground, α_{TD} is the angle of attack for each leg, this is, the aperture that the leg has when it starts the double support phase. In this example, a step occurs when the system passes from single support to double support and a stride is defined when the leg becomes aligned with the toe, this is , the leg returns to it's vertical leg orientation

This model is energetically conservative, therefore, the energy E is a constant with

$$E = \frac{k(l_0 - y_n)^2}{2} + mgy_n + m\frac{v_n^2}{2}. \tag{11}$$

We can express the absolute value of the velocity in terms of the energy. In this model, the only parameters in the initial conditions that can alter the stability of the system for a certain angle of attack α, and energy E are β_0, the angle of the initial velocity with the ground and y_0, the initial vertical position of the CoM.

By allowing the simulation to run over one stride/step, we can associate a map, which is called the Poincaré map, by defining a function A which iterates the Poincaré section, $\psi_n = (y_n, \beta_n)$, this way,

$$\psi_{n+1} = A\psi_n. \tag{12}$$

By recurrence we can apply the A function $n+1$ times from the initial state ψ_0 to get to the final step $n+1$. Not all solutions are admited, if in any instance, the CoM ends up falling this is, $y < 0$, or starts walking backwards, $v_x < 0$, or the leg leaves the ground, $y > l_0$, the set of initial parameters is rejected as a possible stable combination.

3 Simulation Results (walking model)

In this section a method to analyze the stability of the system is displayed regarding the model in section (2.2). The fourth order Runge-Kutta method [2] was applied in order to simulate the Eqs. (5)-(8). A different time steps were used for different situations.

3.1 Fixed points

We are interested in determining the fixed points of the system, this is, the points which repeat after an iteration for a grid of associated parameters. This way, we determine the Poincaré section which we will define by, instead of $\psi_n = (y_n, \theta_n)$, as $\psi_n = (y_n, \Delta x_n)$ [1] and the subsequent Poincaré section $\psi_{n+1} = (y_{n+1}, \Delta x_{n+1})$. Some of the parameters were kept fixed such as the spring stiffness $k = 14000$ N/m, the spring rest length $l_0 = 1$ m, the mass, $m = 80$ Kg and the angle of the initial velocity at VLO $\beta = 0$.

The grid in which the model was studied consists on the variation of 3 parameters, the energy E which changes the initial velocity of the leg and has a variation in the interval $[800, 840]$ J with $\Delta E = 1$J, the angle of attack α which changes the aperture of the leg and it was studied by dividing the interval $[\pi/2 - \pi/5, \pi/2]$ rad into 30 subintervals to access each angle in this range. Also, the initial position y_0 was studied by dividing the interval $[l_0 \sin\theta, l_0]$ into 25 subintervals. This way the parameter space contains $40 \times 30 \times 25 = 30000$ possible configurations in which the system can be stable. Out of all of this possibilities a filtering was applied based on which configurations had successfully completed 2 strides with a time step on the Runge-Kutta of $\Delta t = 0.001$ s.

The criteria for failling to complete a simulation is the same as in the previous section (2.2),this is, configurations in which the center of mass falls ($y < 0$) or goes backwards ($v_x < 0$) or leaves the ground ($y > l_0$), were not suitable as valid candidates for stable configurations of the system. The results of this filtering were that 8195 out of 30000 configurations had successfully completed 2 strides and were selected as candidates for fixed points.

Having this subset of fixed point candidates, configurations in which the differences $|\Delta x_2 - \Delta x_1| < 0.001$, $|(y_1 - y_0)| < 0.001$ and $(y_2 - y_1)| < 0.001$ were elligible as fixed points. After determining the fixed points, it is important to know if they are associated with a stable or unstable region. We can do this by determining the eigenvalues of the Jacobian matrix [8],

$$J = \begin{bmatrix} \frac{\partial \Delta x_{n+1}}{\partial \Delta x_n} & \frac{\partial \Delta x_{n+1}}{\partial y_n} \\ \frac{\partial y_{n+1}}{\partial \Delta x_n} & \frac{\partial y_{n+1}}{\partial y_n} \end{bmatrix}, \tag{13}$$

where each derivative can be computed by the following expression,

$$\frac{\partial \Delta x_{n+1}}{\partial \Delta x_n} = \frac{\frac{\partial \Delta x_{n+1}}{\partial t}}{\frac{\partial \Delta x_n}{\partial t}}. \tag{14}$$

If the eigenvalues of the fixed point lie in the circle of radius 1, this is, if $|\lambda_{1,2}| < 1$, then the fixed point is considered stable, otherwise, is considered a unstable point [13]. With this, in the subset of 8195 configurations which completed 2 strides, 11 were selected as fixed points, in Table (1) the parameters for this points are displayed aswell as the respective eigenvalues of matrices (13).

[1] The definition of the Poincaré section is done this way because the difference in length of the stride provides a more accurate measurement on the fixed points

Energy[J]	α_0	y_0[m]	λ_1	λ_2	Stability
800	1.215	0.950	0.629	0	Stable
801	1.152	0.962	1.711	0	Unstable
809	1.131	0.970	1.388	0	Unstable
812	1.236	0.953	1.860	0	Unstable
814	1.131	0.973	1.144	0	Unstable
821	1.089	0.982	0.536	0	Stable
825	1.110	0.983	1.044	0	Unstable
827	1.236	0.947	-1.063	0	Unstable
828	1.089	0.986	0.734	0	Stable
834	1.089	0.991	0.739	0	Stable
839	1.068	0.995	0.467	0	Stable

TABLE 1: Fixed points table regarding the walking model. In this table we can see that if the energy is higher, the points with higher stability will be those with smaller angles, otherwise the case is reversed.

3.2 Step incrementation

Having determined the fixed points and their respective type, an estimation of the stable and unstable zones of the parameter space was determined. This was done by incrementing the step of the configurations that completed 2 strides (3.1), so that the maximum number of steps,*maxsteps*, increases by 1 from [3,10] with a Runge-Kutta time step of $\Delta t = 0.00075$ s. If the simulation registered a success when the step was incremented, we increment another step, otherwise, we associate to that configuration a maximum number of steps of $maxsteps - 1$. If a configuration point reached 10 steps, we registered the number of steps to that configuration to be *maxsteps*. Fig. (3) shows the final result obtained aswell with the points that succeeded 10 steps as the fixed points associated.

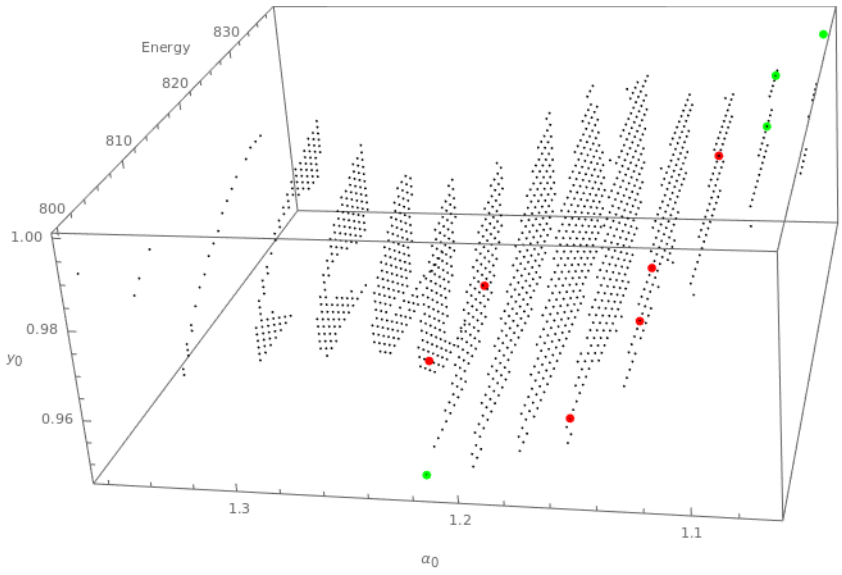

FIGURE 3: Successful 10 step configurations with stable fixed points in green and unstable fixed points in red. In this 3D plot the Energy was varied from 800 and 840, y_0 from 0.8 to 1 and α_0 from 0.94 to 1.57 and only this configurations remained. The fixed points displayed are associated to Table (1). There is a preference for the stable configurations to have angle of attack of $\approx$ [1.05,1.25]

Figures (4) and (5) simulate the behaviour of the Center of Mass in the walking model for respectively a stable and an unstable fixed point a constant angle of attack policy.

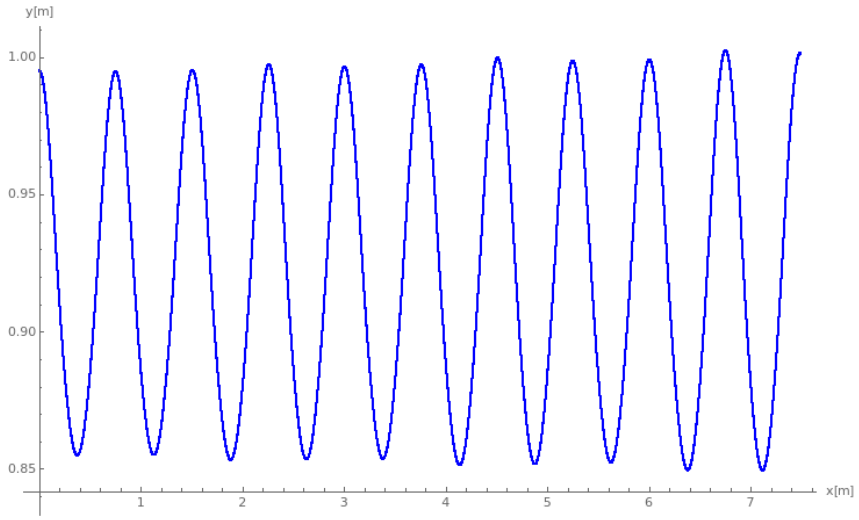

FIGURE 4: Position of the CoM of the stable fixed point E=839J, α_0= 1.068,y_0=0.995, Runge-Kutta timestep $\Delta t = 0.0005$s. In this example, the fixed point successfully covers all 10 strides with no instability.

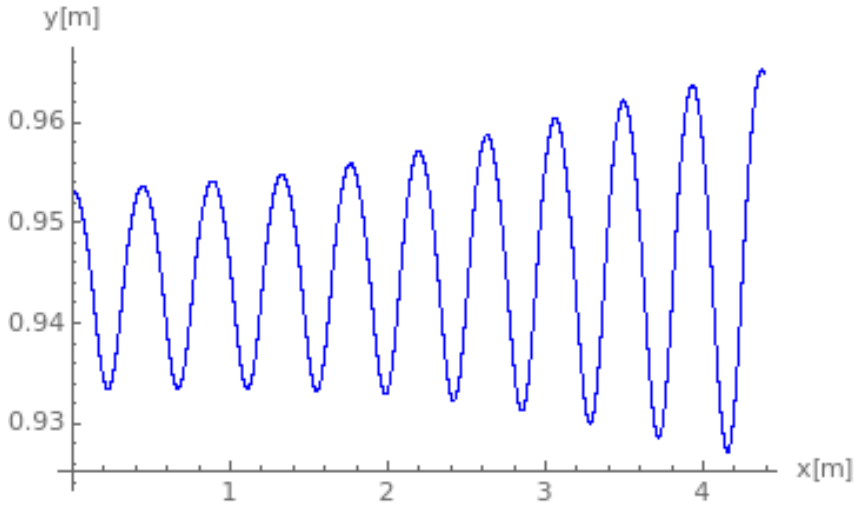

FIGURE 5: Position of the CoM of the unstable fixed point E=812J, α_0= 1.236,y_0=0.953, Runge-Kutta timestep $\Delta t = 0.0005$s. In this example, the fixed point successfully covers all 10 strides, but the amplitude increases in each stride bringing the system to an unstable configuration.

4 Future Work

4.1 Touch-down angle of attack control strategy

Although in sections (2.2) and (3) a constant angle of attack policy was introduced, it is possible to have a dynamical control of this parameter so that after 2 strides the system is found in a stable setup. As discussed in [5], a single step correction is insufficient for the system to have a stable walking gait. Therefore, by implementing a two step control policy, we have ensured stable walking in the

minimum number of steps. Such type of control is also called deadbeat control policy. This is done in [14], using a feedback control technique that sends the next step of the system into a stable walking gait.

Supposing we have an equilibrium state (ψ^*, θ^*) which we want to achieve. We can find the two stride region of attraction (y, β) if we find a state ψ_n which satisfies,

$$A(\psi_n, \theta_n) = \psi_{n+1}, \tag{15}$$

$$A(\psi_{n+1}, \theta_{n+1}) = \psi^*. \tag{16}$$

If Eqs. (15) and (16) are satisfied, the system will converge to ψ^* in the fastest number of steps (deadbeat control policy). This way, the angle that is chosen for the next iteration is given through the invertion of the poincare section combination found, this is,

$$\theta_n = A^{-1}\Big|_{\psi_n}(\psi_{n+1}) \tag{17}$$

where the existence of a valid intermediate state ψ_{n+1} is assured by constructing a two-step domain. Notice that eventhough it is necessary to obtain a value for θ_{n+1} to compute $A(\psi_{n+1}, \theta_{n+1})$, in practice, this value is not used to compute the next iteration of angle of attack but to filter the states in which $A(\psi_{n+1}, \theta_{n+1}) = \psi*$.

4.2 2 spring model for running and walking

To contemplate a more realistic model, throught this thesis I plan to develop a more realistic model for running, robust to noise. It consists on two springs with spring stiffness k_1 and k_2, and 3 masses, m_1, m_2, m_3, the angle velocity makes with the ground is defined by γ_0 and $\vec{v_0}$ is the initial velocity vector. Figs. (6)-(8) displays the 3 control phases and important variables to this new model.

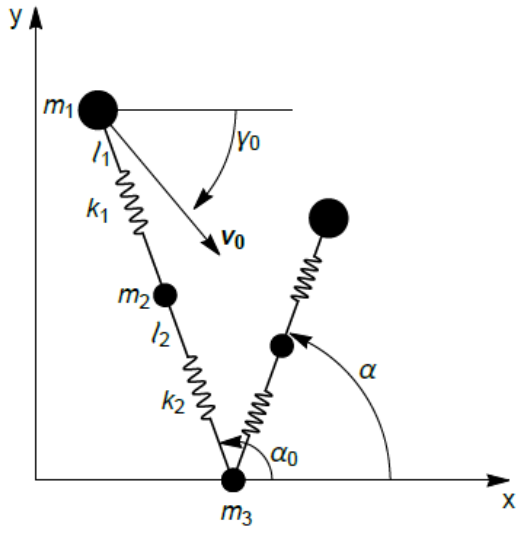

FIGURE 6: Phase-I of the 2 spring model, ground phase to aerial phase. With no bending, the leg rotates around it's pivot located on the ground similar to section (2.1). Upon reaching the angle α the model starts the phase II, aerial phase.

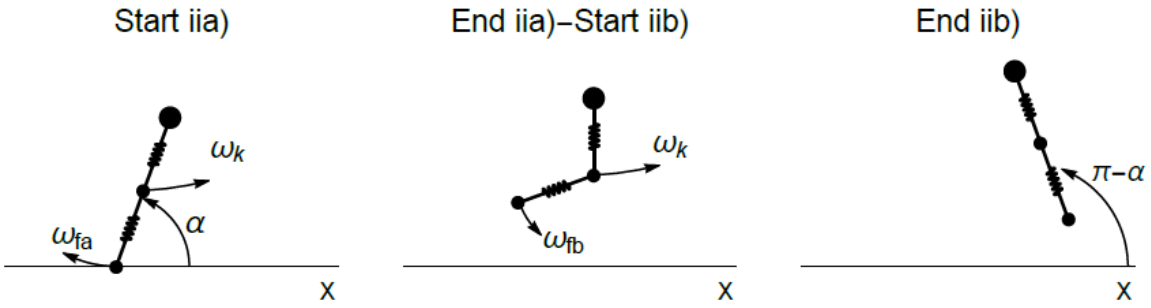

FIGURE 7: Phase-II of the 2 spring model, aerial phase. Part a) of this phase involves rotating the rotor in the joint, so that a torque is applied to the second part of the leg making it move in the clockwise orientation. At the same time, a torque is also applied to the first part of so making it rotate in a counter-clockwise orientation. With this, when the first part of the leg reaches it's vertical orientation the second part of this phase starts. Part b) is about moving the leg so that it becomes aligned with with an angle of $\pi - \alpha$.

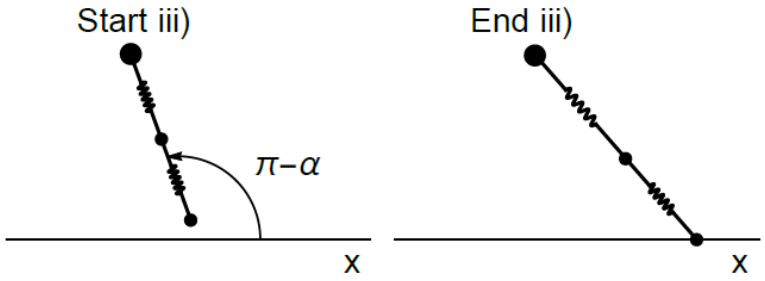

FIGURE 8: Phase III of the 2 spring model, aerial phase to ground phase. With the leg extended, free fall starts so that the leg contacts the floor so that phase I starts again.

Using a similar kind of mechanism to section (4.1), I pretend to make a model which is capable of finding the region of attraction so that it is adaptative to initial conditions and obstacles such as stairs and other kind of irregular surfaces. This way, one of the objectives will be to analyze the stability of the parameters described, this is, the strong and weak points of this model.

Besides a running model, I will also plan to implement a walking model with joints but with double support and single support phases similar to the case of section (2.2).

5 Work schedule

In this section with Table 2 I present an overview of the work to be done throught this thesis.

	Fev	Mar	April	May	June	July	August	Sept
Refining the stability analysis of the two legs walking model								
Development and analysis of the one leg two-springs model (walking and running)								
Development and analysis of the two leg two-springs model (walking and running)								
Thesis writting								

TABLE 2: Summary of the work to be done throught the thesis

References

[1] R McN Alexander. "Mechanics of bipedal locomotion". In: *Zoology*. Elsevier, 1976, pp. 493–504.

[2] George B Arfken and Hans J Weber. *Mathematical methods for physicists*. 1999.

[3] Reinhard Blickhan. "The spring-mass model for running and hopping". In: *Journal of Biomechanics* 22.11-12 (1989), pp. 1217–1227.

[4] GA Borelli. "De Motu Animalium, 1680-1". In: 1685.

[5] Sean G Carver, Noah J Cowan, and John M Guckenheimer. "Lateral stability of the spring-mass hopper suggests a two-step control strategy for running". In: *Chaos: An Interdisciplinary Journal of Nonlinear Science* 19.2 (2009), p. 026106.

[6] Giovanni A Cavagna, H Thys, and A Zamboni. "The sources of external work in level walking and running." In: *The Journal of Physiology* 262.3 (1976), pp. 639–657.

[7] Robert J Full and Daniel E Koditschek. "Templates and anchors: neuromechanical hypotheses of legged locomotion on land". In: *Journal of Experimental Biology* 202.23 (1999), pp. 3325–3332.

[8] Hartmut Geyer, Andre Seyfarth, and Reinhard Blickhan. "Compliant leg behaviour explains basic dynamics of walking and running". In: *Proceedings of the Royal Society of London B: Biological Sciences* 273.1603 (2006), pp. 2861–2867.

[9] Thomas A McMahon and George C Cheng. "The mechanics of running: how does stiffness couple with speed?" In: *Journal of Biomechanics* 23 (1990), pp. 65–78.

[10] Simon Mochon and Thomas A McMahon. "Ballistic walking". In: *Journal of Biomechanics* 13.1 (1980), pp. 49–57.

[11] Marcus G Pandy. "Simple and complex models for studying muscle function in walking". In: *Philosophical Transactions of the Royal Society of London B: Biological Sciences* 358.1437 (2003), pp. 1501–1509.

[12] Juergen Rummel, Yvonne Blum, and Andre Seyfarth. "Robust and efficient walking with spring-like legs". In: *Bioinspiration & biomimetics* 5.4 (2010), p. 046004.

[13] Steven H Strogatz. *Nonlinear Dynamics and Chaos: With Applications to Physics, Biology, Chemistry, and Engineering (Boulder, CO)*. 2001.

[14] Hamid Reza Vejdani et al. "Touch-down angle control for spring-mass walking". In: *2015 IEEE International Conference on Robotics and Automation (ICRA)*, IEEE. 2015, pp. 5101–5106.